Synthesis of CuO/SnO_2 NPs on quartz substrate for temperature sensors application

D. Faisal[a], W. K. Kalef[b], E. T. Salim[b,*], F. H. Alsultany[c]
[a] *Ibn khaldun privte university college -Iraq*
[b]*University of Technology-Iraq, Department of Applied Science, , Baghdad, Iraq*
[c]*Al-Mustaqbal university collage, Department of Medical Physics, Iraq*

Temperature sensor of p-CuO/n-SnO_2 heterojunction was successfully fabricated and investigated. SnO_2 nanostructure was firstly synthesized via chemical vapor deposition. Followed by a top layer of CuO nanoparticles was deposited on SnO_2 by drop cast method. The SnO2 film was analyzed via x-ray diffraction (XRD) and scanning electron microscope (SEM). The XRD confirms the formation of the SnO_2 nanstructure .The SEM reveals the SnO_2 nanoparticles agglomerated together forming a cauliflowers-like nanostructure with a calculated particle size of 17nm. The temperature response corresponding to the relative variation of sensor resistance (ΔR) to a given temperature was measured. It was found that the present sensor has a high sensitivity of 0.56%/°C. Temperature sensor p-CuO/n-SnO_2 heterojunction was found to be quite promising material in the temperature range of 25-200° C.

(Received December 29, 2021; Accepted April 1, 2022)

Keywords: Tin oxide nanoparticles (SnO_2 NPs), Temperature sensor, Heterojunction, Copper oxide nanoparticles (CuO NPs), Sensor sensitivity

1. Introduction

Metal oxides, SnO_2 is an important n-type wide-energy-gap semiconductor (E_g = 3.64 eV, 330 K) ,which has a wide range of applications such as in solid-state gas sensors [1], transparent conducting electrodes [2], rechargeable Li batteries [3], and optical electronic devices [4].Many processes have been developed to the synthesized SnO_2 nanostructures, such as spray pyrolysis [5] , hydrothermal methods [6-8]. Also,evaporating tin grains in air [9]. SnO_2 has been widely used to detect combustible and toxic gases. Tin oxide nanowires (SnO_2 NWs) grown on quartz and silicon substrates via a chemical vapor deposition (CVD) and fabricated as an ethanol gas sensor was recently reported [10]. Thermal evaporation of oxide powders [11], rapid oxidation tin metal [12], sol–gel method [13], etc. Highly crystalline SnO_2 nanowires has been also synthesized and functionalized with copper particles using a CVD technique [14]. Controlled oxidation of Cu to CuO led to the formation of CuO/SnO_2 p–n heterojunctions, which were found to be highly sensitive and selective towards the detection of H_2S gas. There are many uses of tin oxide as mainly as a gas sensor as mentioned previously by Khalef Wafaa Khalid et.al [15]. It can also fabricate as temperature sensor, other metal oxides also fabricated as a temperature sensor such as [16]. In the present work, we were focused on the CuO/SnO2 As A temperature sensor in at an attempted range of 20-200c.

2. Experimental procedure

The quartz substrates were firstly cleaned by sonication in deionized water for 15 minutes. Then they were immersed in a beaker containing isopropyl alcohol in an ultrasonic cleaner for about 15min. Finally, quartz substrates were flushed by a jet of nitrogen gas, then they were dried in the oven for 30 minutes. The CuO/SnO_2 was grown in two steps:

1st step: SnO_2 nanostructure was synthesized via chemical vapor deposition (CVD) technique. Sn powder of 1g was loaded into small ceramic boat with quartz substrate positioned at 1cm from the powder. This ceramic boat was inserted in a middle of quartz tube of two opened

[*] Corresponding author: evan_tarq@yahoo.com

https://doi.org/10.15251/JOR.2022.182.205

ends. Argon and oxygen gases were introduced from the left side and water bubble was fixed at the outlet end. Firstly, Argon was introduced with a flow of 100sccm for 15 minutes to clean the quartz tube and then the temperature was raised with rate of 25° C/minute up to 900° C, then oxygen gas was introduced with a flow of 5sccm for 1h.

2nd step: copper oxide (CuO) was deposited using drop cast method on the SnO_2 nanostracture film growth via chemical vapor deposition (CVD). Copper oxide nanoparticles (NPs) was prepared by dissolving 30 mM (0.054 g) of copper acetate (Cu_2 $(CH_3COO)_4$) in 10 ml of deionized water (DI). The solution was sonicated for 15 minutes to insure the dissolving of copper acetate in the water. Afterwards, a micro-pipette was used to drop the solution of 30 µL on the surface of the pre-synthesized SnO_2 on quartz substrates. The coated material was subsequently dried onto a hot plate at 150℃ for 5 minutes. These coating steps were repeated four times to insure the formation of CuO NPs on the SnO_2 film. The final product should be CuO/SnO_2 films prepared on quartz substrates.

3. Result and discussion

3.1. XRD analysis

XRD pattern was analyzed using X-ray diffractometer (Shimadzue 6000 / Japan) with CuK_α (λ= 0.15406 nm) radiation. Fig. 1 shows the XRD pattern of SnO_2 synthesized by CVD. This pattern shows a polycrystalline structure with three strongest peaks at 2Θ=26.9821° , 34.2641° , and 52.1476° . These peaks belongs to the (110), (101), and (211), respectively. There are other small peaks belongs to the same structure. The analysis indicates that the synthesized material is pure and less crystalline. Due to the XRD analysis, it was found that the results were comparable to the SnO_2 standard data of JPDFS # 41-1445.

The average crystallite size value of SnO_2 nanoparticles was calculated using Debye-Scherrer's formula as below [17]:

$$D=0.9\lambda / \beta\cos\Theta \tag{1}$$

where D, λ, β, and Θ are the crystallite size, x-ray wavelength, full width at half maximum (FWHM) , and Bragg's angle, respectively. So, the calculated value of the SnO_2 crystallite size is 17nm±0.8. This value is small and confirm the nanostructure formation. The lattice parameters a, and c for SnO_2 was calculated using the following equation [18]

$$1/d^2=\{(h^2+k^2)/a^2\}+l^2/c^2 \tag{2}$$

The standard values of a and c for SnO_2 were a=4.737Å and c= 3.185Å. Where the calculated values of the present structure are a= 4.670Å, and c=3.156Å. It was also compared with the data of other workers [19-20]. These data are presented in Table 1.

Table 1. Lattice parameters calculated data for SnO_2NPs.

Lattice parameters	Present work	Standard (JPDFS # 41-1445)	References	
			[19]	[20]
a (Å)	4.670	4.737	4.687	4.765
c (Å)	3.156	3.185	3.161	3.1843

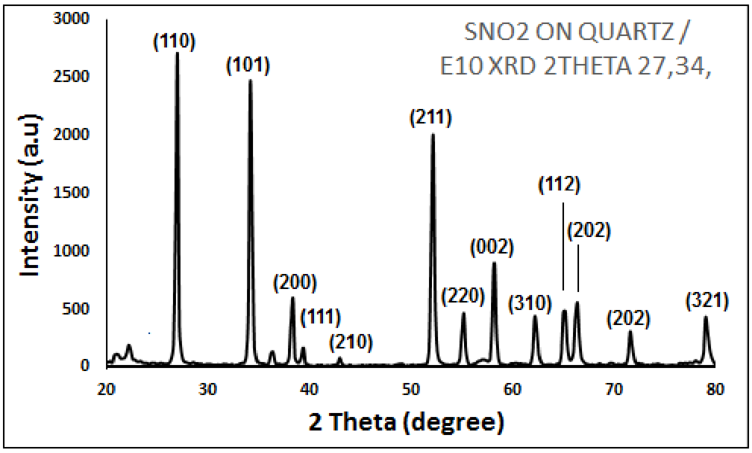

Fig. 1. XRD pattern of SnO_2 on quartz substrate.

3.2. SEM analysis

The morphology of SnO_2 nanostructure on quartz substrate was analyzed by using scanning electron microscope (SEM / FEI Inspect S50 /Netherland). Figure 2 shows SEM images at various magnifications. These images reveal the SnO_2 nanoparticles agglomerated together forming a cauliflowers-like nanostructures. It covers a large area on the quartz substrate as shown in Fig. 2a. The average size of SnO_2 nanoparticles was calculated previously from the XRD data. Small particle size within 17nm was found.

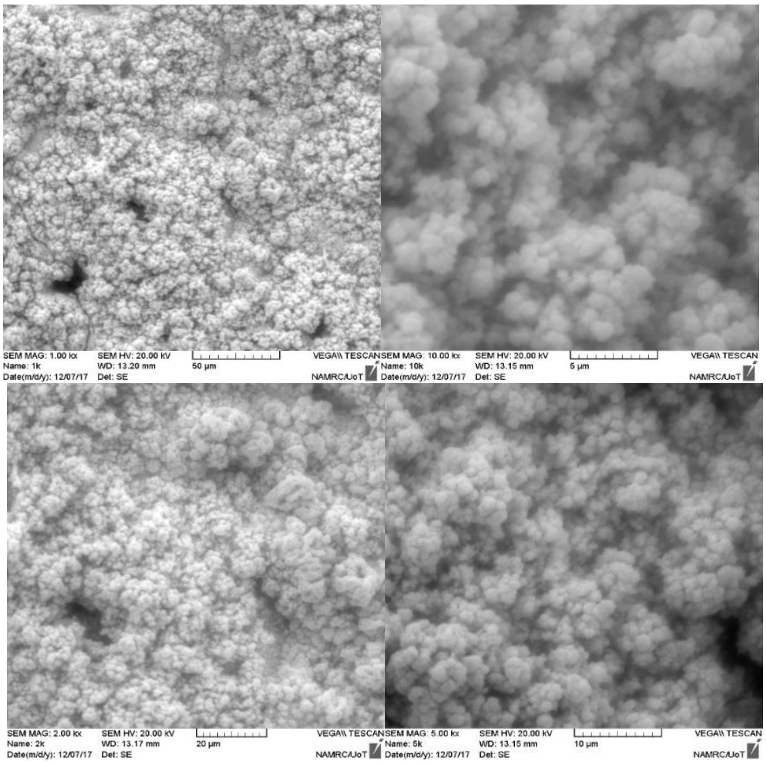

Fig. 2 SEM images at various magnifications (a) 50, (b) 20, (c) 10, and d) 5μ m for SnO_2 NP's (cauliflower-like nanostructure) on quartz substrates.
SEM and EDS of CuO/SnO_2/ quartz

Figure 3 shows a typical SEM image of CuO/SnO_2 nanostructures at various magnifications. The elemental spectrum of of CuO/SnO_2 structures shown in Fig.3 is explained in the Energy Dispersive Spectroscopy as shown in Fig.4 with the corresponding elemental data. The EDS spectrum is clearly shows the Sn, Cu, and O elements.

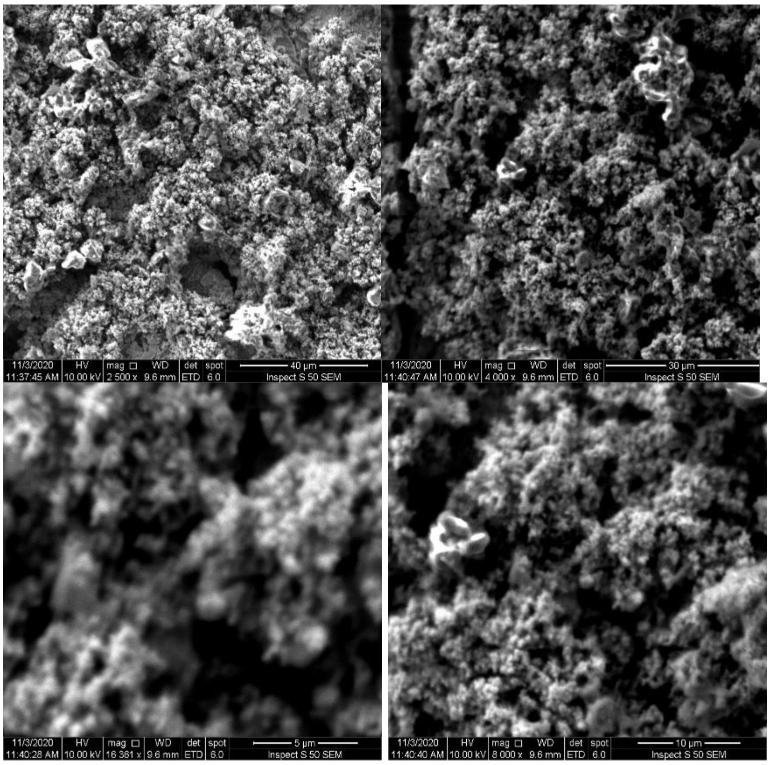

Fig. 3 SEM of CuO/SnO_2/ quartz.

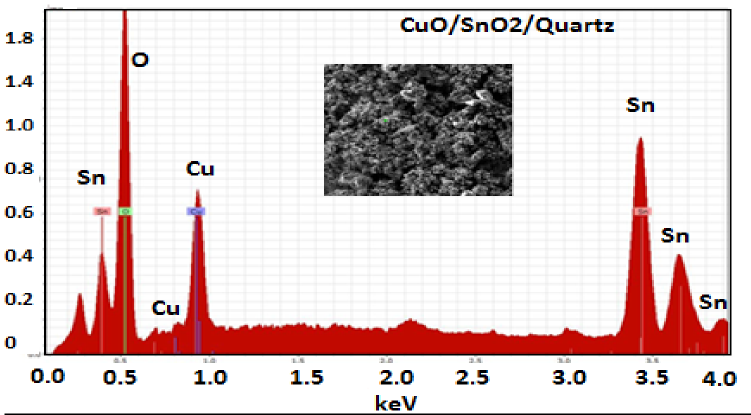

EL	AN	Series	unn. C (wt.%)	nom. C (wt.%)	Atom. C (at.%)	Error (1 Sigma) (wt.%)
Sn	50	L-series	45.34	54.35	19.67	1.57
O	8	K-series	20.55	24.63	66.13	2.82
Cu	29	L-esries	17.52	21.01	14.20	2.63
		Total :	83.41	100.00	100.00	

Fig. 4. EDS of CuO/SnO_2/ quartz with corresponding elemental analysis.

3.3. Temperature Sensor Fabrication

The temperature sensor was fabricated based on p-CuO/ n-SnO_2 materials on quartz substrates. Fig. 3 demonstrate the sensor device. The two arrows represent the probes used for the electrical and thermal measurements. I-V characteristics of p-CuO/n-SnO_2 in the dark was firstly measured as shown in Fig.4. The observed curve indicates a rectification phenonmenon. This is reflected the contacts of n and p type of semiconductor materials.

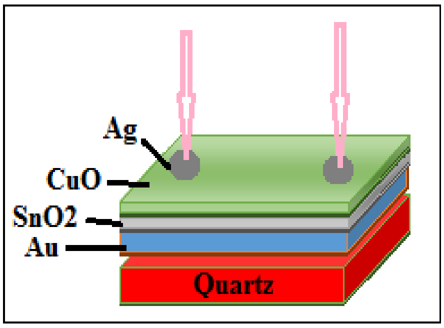

Fig. 5. Fabrication of the temperature sensor device of CuO/ SnO_2/quartz.

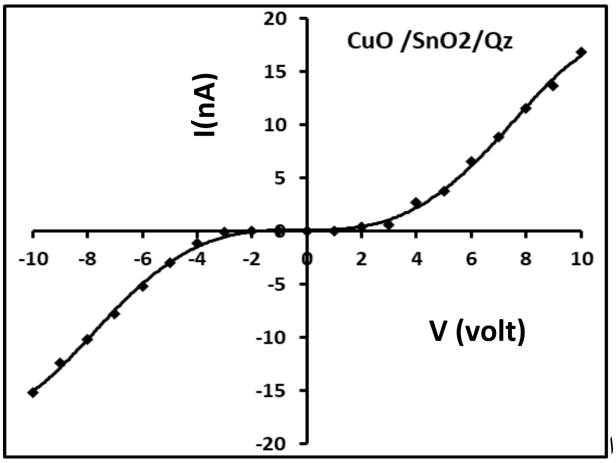

Fig. 6. I-V characteristic of CuO /SnO_2/Qz in the dark.

3.4. Thermal measurements of CuO /SnO_2

The resistance of the sensing device was measured as a function of temperature in the range of 25-200ºC. This measurement is plotted as shown in Fig.7. The data were fitted to an exponential curve with the fitting formula of:

$$y=0.0431e^{-(0.008x)} \tag{3}$$

Regarding to the fitting formula represented in equation (3), it was compared with the exponential formula of the resistance [21].

$$R_t = R_o\, e^{-(\alpha\, \Delta T)} \tag{4}$$

where R_o, R_t, α, Δ T are the resistance at 0°C, resistance at a certain temperature, thermal coefficient, and temperature difference, respectively. So, the obtained value of R_o is 0.0431MΩ and α=-0.008/°C. The minus sign means that the resistance is exponentially decreasing when the temperature increased. Figure 6 shows a linear relation between $\ln R/\ln R_o$ versus the temperature. The slope of the linear fitting relation represents the temperature coefficient =0.0083/°C.

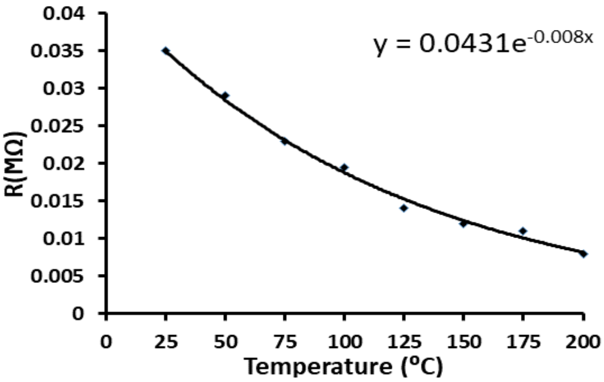

Fig. 7. Resistance versus temperature of CuO /SnO_2/Qz at air.

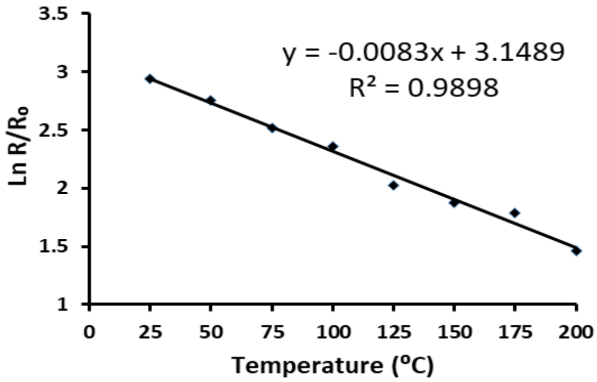

Fig. 8. Ln R/R_0 versus temperature of CuO /SnO_2/Qz.

3.5. Temperature Sensitivity

The temperature sensitivity is an essential factor to evaluate the sensor performance, which is based on temperature variation. Firstly the sensor's response and its sensitivity are investigated. The resistance of the sample exponentially decreased with increasing temperatures over the range as previously shown in Fig. 5. The temperature response can be given in terms of relative variation (ΔR) of the sensor resistance to a given temperature, [22]:

$$\Delta R=[R_o - R_t / R_o]/ \text{ x } 100\% \quad (5)$$

where R_o and R_t are the initial resistance and the resistance of the sensor at different temperature, respectively.

The variation of ΔR versus temperature was plotted in the range from 25-200°C is shown in Fig. 7. The sensitivity of this device is determined from the slope of ΔR. The highest sensitivity ($S= \Delta R / R_o \Delta T$) value of 0.56%/1°C was calculated from Fig. 7. The average value of the resistance change per 1 °C in the temperature range of 25-200°C was equal to150Ω/°C.

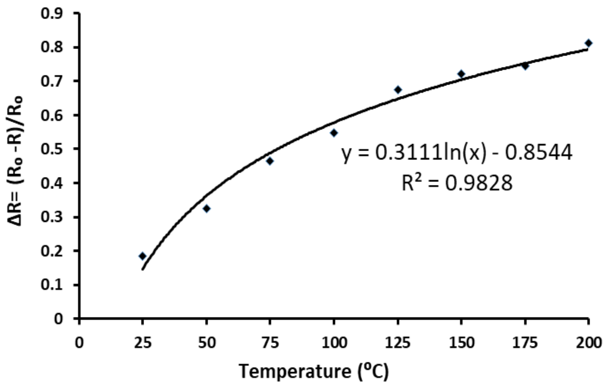

Fig. 9. Variations of ΔR versus temperature of CuO /SnO_2.

Table 2. Temperature sensor measurements of CuO/SnO_2 film.

T(°C)	R (MΩ)	R (kΩ)	$\Delta R = [(R_o - R)/R_o]$ /%	R_o (kΩ)
25	0.035	35.0	18.8	43.1
50	0.029	29.0	32.7	
75	0.023	23.0	46.6	
100	0.0195	19.5	54.8	
125	0.014	14.0	67.5	
150	0.012	12.0	72.2	
175	0.011	11.0	74.5	
200	0.008	8.00	81.4	

5. Conclusion

The hetrojunction metal oxides of p- CuO/n-SnO_2 were synthesized via CVD and drop cast methods. The structure and morphology of the films were investigated by SEM and XRD. The electrical and thermal properties were measured and confirmed a semiconductor properties.

These films was successfully fabricated as a promising temperature sensor based on CuO/SnO_2 and exhibit a maximum sensitivity in the temperature range of 20-200° C.

References

[1] Ying, Z., Wan, Q., Song, Z.T., Feng, S.L, Nanotechnology 15, 1682 (2004); https://doi.org/10.1088/0957-4484/15/11/053
[2] Chopra, K.L., Major, S., Pandya, D.K., Thin Solid Films 102, 1 (1983); https://doi.org/10.1016/0040-6090(83)90256-0
[3] Peng, Z., Shi, Z., Liu, M., Chem. Commun. 21, 25 (2000); https://doi.org/10.1039/b007687m
[4] Aoki, A., Sasakura, H., Japan J. Appl. Phys. 9, 582 (1970); https://doi.org/10.1143/JJAP.9.582
[5] Paraguay-Delgado, F., Antúnez-Flores, W., Miki-Yoshida, M., Aguilar- Elguezabal, A., Santiago, P., Diaz, R., Ascencio, J.A. Nanotechnology 16, 688 (2005); https://doi.org/10.1088/0957-4484/16/6/011
[6] Cheng, B., Russell, J.M., Shi, W., Zhang, L., Samulski, E.T.: Large-scale, J. Am. Chem. Soc. 126, 5972 (2004); https://doi.org/10.1021/ja0493244
[7] Du, F., Guo, Z., Li, G., Mater. Lett. 59, 2563 (2005); https://doi.org/10.1016/j.matlet.2005.03.046
[8] Fujihara, S., Maeda, T., Ohgi, H., Hosono, E., Imai, H., Kim, S., Langmuir 20, 6476 (2004); https://doi.org/10.1021/la0493060

[9] Duan, J., Yang, S., Liu, H., Gong, J., Huang, H., Zhao, X., Zhang, R., Du, Y., J. Am. Chem. Soc. 127, 6180 (2005); https://doi.org/10.1021/ja042748d
[10] Khalid, Khalef Wafaa, Aljubouri Ali Abadi, Faisal Abdulqader Dawood, Journal of Inorganic and Organometallic Polymers and Materials 30.9 (2020): 3294-3304; https://doi.org/10.1007/s10904-020-01617-3
[11] Dai, Z.R., Gole, J.L., Stout, J.D., Wang, Z.L., T J. Phys. Chem. B 106, 1274 (2002); https://doi.org/10.1021/jp013214r
[12] Hu, J.Q., Ma, X.L., Shang, N.G., Xie, Z.Y., Wong, N.B., Lee, C.S., Lee, S.T., J. Phys. Chem. B 106, 3823 (2002); https://doi.org/10.1021/jp0125552
[13] Pourfayaz, F., Khodadadi, A., Mortazavi, Y., Mohajerzadeh, S.S., Sensors Actuators B108, 172 (2005); https://doi.org/10.1016/j.snb.2004.12.107
[14] Giebelhaus, Irina, Elena Varechkina, Thomas Fischer, Marina Rumyantseva, Vladimir Ivanov, Alexander Gaskov, Joan Ramon Morante, Jordi Arbiol, Wieland Tyrra, Sanjay Mathur, Journal of Materials Chemistry A 1, no. 37 (2013): 11261-11268; https://doi.org/10.1039/c3ta11867c
[15] Khalef Wafaa Khalid, Aljubouri Ali Abadi, Faisal Abdulqader Dawood, Journal of Inorganic and Organometallic Polymers and Materials
[16] Ali A. Aljubouri, Abdulqader D. Faisal, Wafaa K. Khalef, Materials Science-Poland, 36(3), 2018, pp. 460-468; https://doi.org/10.2478/msp-2018-0051
[17] S. Chacko, N.S. Philip, K.G. Gophandran, P. Koshy, V.K. Vaidyan, 254, 2179-2186, Appl. Surf. Sci. 2008; https://doi.org/10.1016/j.apsusc.2007.09.027
[18] R.R. Kasar, N.G. Deshpande, Y.G. Gudage, J.C. Vyas, R. Sharma, 403, pp. 3724-3729, Physica B 2008; https://doi.org/10.1016/j.physb.2008.06.023
[19] S. P. Choudhury, N. Kumari, A. Bhattacharjee, UGC Sponsored National Seminar on Emerging Trends in Plasma Technology and Its Applications (ETPTA-2014), 20-21 August 2014, Sri Vasavi College, Erode – 638316, India
[20] Ning Wan, Xia Lu, Yuesheng Wang, Weifeng Zhan, Ying Bai, Yong-Sheng Hu. Sheng Dai, Scientific Reports 6:18978 January 2016, https://doi.org/10.1038/srep18978
[21] Richa Srivastava, Journal of Sensor Technology 02(01), January 2012; https://doi.org/10.4236/jst.2012.21002
[22] A. Croft, T. Croft, R. Davison, M. Hargreaves, Engineering Mathematics: a Modern Foundation for Electronic, Electrical, and Control Engineers, Addison- Wesley, London, 1992.